dition. The reflection boundary condition (RBC) and the absorbing boundary condition (ABC) are examples of such velocity boundaries that have been investigated with the problem of synthesizing a rectangular deep null in the sidelobe region. The obtained results show that by using an RBC or ABC, and then carefully choosing V_{max}, it is possible to arrive at a much better convergence performance, as compared with those of the traditional soft boundary condition and the velocity-clipping criterion that uses the value of V_{max} equal to the maximum dimension of the problem. Thus, the importance of V_{max} increases with the incorporation of these boundary-condition types.

REFERENCES

1. J. Kennedy and R.C. Eberhart, Particle swarm optimization, Proc IEEE Conf Neural Networks IV, Piscataway, NJ, 1995.
2. J. Robinson and Y. Rahmat-Samii, Particle swarm optimization in electromagnetics, IEEE Trans Antennas Progat 52 (2004), 397–407.
3. D. Boeringer and D. Werner, Particle swarm optimization versus genetic algorithms for phased array synthesis, IEEE Trans Antennas Progat 52 (2004), 771–779.
4. J.R. Perez and J. Basterrechea, Particle-swarm optimization and its application to antenna far field-pattern prediction from planar scanning, Microwave Opt Technol Lett 44 (2005), 398–403.

PROGRAMMABLE HIGH-SPEED TRUE-TIME-DELAY OPTICAL PROCESSOR FOR PHASED-ARRAY ANTENNAS USING A RECIRCULATING LOOP

Xueyan Zheng, Sergio Granieri, and A. Siahmakoun
Department of Physics and Optical Engineering
Rose-Hulman Institute of Technology
5500 Wabash Ave., Terre Haute, IN 47802

Received 9 March 2005

ABSTRACT: *A programmable high-speed true-time-delay (TTD) processor using a recirculating loop is proposed for optical beamforming and phased-array antennas. The number of TTD elements is reduced by several times, in comparison to other methods. The reconfiguration time of beamsteering can reach tens of nanoseconds. The experimental results for the proof-of-concept of this optical beamformer are presented.* © 2005 Wiley Periodicals, Inc. Microwave Opt Technol Lett 46: 426–429, 2005; Published online in Wiley InterScience (www.interscience.wiley.com). DOI 10.1002/mop.21005

Key words: *true-time delay; phased-array antennas; optical beamforming*

1. INTRODUCTION

There has been significant interest in using optical methods to generate true-time delay (TTD) for phased-array antennas (PAAs). Significant advantages such as light weight, compactness, nondispersiveness over multiple microwave bands, and immunity to electromagnetic interference make photonics systems an attractive option over electronic counterparts. Several approaches have been proposed, including fiber delay lines [1, 2], wavelength division multiplexing architectures [3, 4], fiber Bragg gratings [5, 6], acousto-optic modulators [7], optoelectronics-integrated circuits [8], and free-space approaches [9, 10]. However, all of the proposed methods need either a large number of TTD elements to realize large-scale PAAs or operation at a low steering speed.

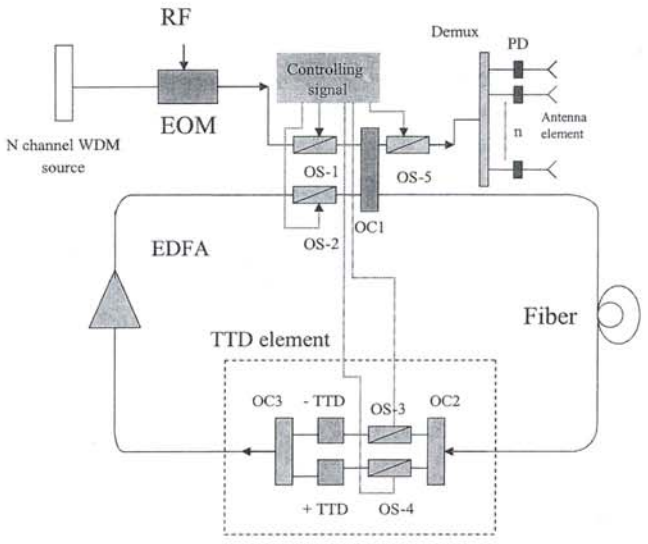

Figure 1 TTD optical beamformer architecture for transmit mode based on a recirculating loop (OS: optical switch, OC: optical coupler, PD: photo detector; EOM: electro-optic modulator)

In this paper, a high-steering-speed, cost-effective, and programmable TTD processor for PAAs based on an optical recirculating loop is proposed. The steering speed can reach up to nanoseconds based on commercial technologies [11] and the architecture can significantly reduce the amount of TTD elements, as compared to the other methods. The experimental results for a proof-of-concept prototype are also presented.

2. SYSTEM DESCRIPTION

The proposed TTD system is based on the concept of the optical-fiber recirculating loop [12]. Figure 1 shows the schematic of the programmable recirculating loop (PRL). A multiwavelength laser source provides N optical carriers with wavelengths λ_1 through λ_N. These optical channels are externally modulated with an RF signal by an electro-optic modulator. After the modulation stage, the optical signal is inserted into the recirculating loop through the 2×2 optical coupler OC1. Two TTD elements located inside the fiber loop generate a time delay $\pm\tau$ between adjacent channels, resulting in a total time delay of $\pm N\tau$ between channels λ_1 and λ_N. Optical switches OS3 and OS4, along with 2×2 fiber couplers OC2 and OC3, are used to select the time delay between adjacent channels to be either $+\tau$ or $-\tau$. The capability of the loop to produce positive and negative time delays allows the phased-array antenna to be symmetrically steered around the broadside direction for the receive/transmit mode [13]. Optical loses are compensated by introducing an EDFA inside the fiber loop. The loop length is 200 m with a total optical transit time around the loop of ~ 1 μs. The working principles of the proposed processor in transmit mode can be summarized in the following sequence.

- Step 1: OS1 is turned on for the transient time of 1 μs in order to open the input path of the recirculating loop to the modulated optical signal. OS2 and OS5 are off while a positive or negative time delay is selected by setting OS3 and OS4 accordingly.
- Step 2: Once the optical signal with a time window of around 1 μs is in the loop, OS1 is turned off and OS2 is turned on. This allows the recirculation of the signal into the loop. After the signal recirculates M times through the loop, the time delay between adjacent optical channels is $M\tau$ or $-M\tau$,

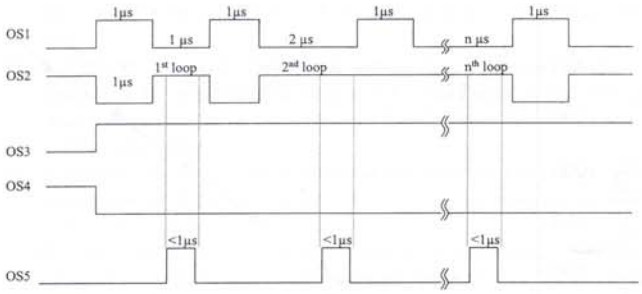

Figure 2 Timing sequence of the optical switches in the PRL

while the maximum time delay along the complete channel spectrum is $MN\tau$ or $-MN\tau$, respectively.

- Step 3: OS5 is used to decide when the delayed optical signal is detected by the photo detectors (PDs). An optical signal with the desired time delay can be obtained at the output of the fiber loop by synchronizing the turn-ON time of OS5 with the transit time of the signal inside the loop. For example, if OS5 is turned on after the first pass for less than 1 μs (in order to avoid the overshooting caused by the OS5), the delay between adjacent channel will be $\pm\tau$ (the sign depends on the positions of switches OS3 and OS4). In the case for which OS5 is turned on, after M loop passes, the delay between adjacent channels becomes $\pm M\tau$.
- Step 4: The output optical signal from the recirculating loop is demultiplexed and each delayed channel is detected by a single PD. Finally, the RF signals out of each PD is fed to the transmit/receive (T/R) elements of the antenna. For continuous steering (for sweeping the direction of the T/R RF-beam), the ON-time of OS5 is incremented by an integral number of transit times (loop periods) in each new sequence until the maximum delay is obtained. Nevertheless, if a fixed delay is needed for a fixed RF-beam direction, the ON-time of OS5 can be set to produce the required time delay.

The time sequence for all five optical switches representing the described procedure is shown in Figure 2. Normally, a certain length of fiber is needed in the loop in order to give the OS enough time to switch and allow the receiver to respond to the optical signal. Any additional dispersion from the optical fiber in the loop can be compensated by using the dispersion-slope compensation technique. Consequently, the fiber will not introduce any undesirable time delay, except for the intended one. The minimum and maximum time delays between adjacent channels are determined by a single pass through the TTD element and the maximum number of loop passes, respectively. Therefore, the time delay can be easily modified without adding any additional TTD device. The steering speed of the PRL is established by the loop length, maximum loop passes, and speed of the optical switches. The maximum number of loop passes is determined by the maximum angular direction of the PAA. The angular direction of the transmitted/received beam is given by $\theta = \arcsin\left[\frac{cM\tau}{\Lambda}\right]$, where τ is the loop delay between adjacent channels, M is the number of loop passes, and Λ is the T/R elements separation in the PAA. A typical radar application requires PAA steering angles from -70° to $+70^\circ$. Therefore, an RF signal at 10 GHz with a typical separation of 1.5 cm between T/R elements and a loop delay of 1 ps results in an angular resolution of about 1° and 3° for broadside and $\pm 70^\circ$, respectively. In this particular case, the maximum number of loop passes is 47 for both positive and negative time delays. Note that the reconfiguration time, that is, the time between two different angular directions, is not uniform. The reason is that in order to set the proper delay for larger angles, that is, larger time delays, more loop passes are needed. For the 200-m loop length, the steering time for the angular positions related to τ and 2τ is ~ 2 μs, and that for 2τ and 3τ is ~ 3 μs, and so on. However, the response time of the OS can reach tens of nanoseconds, based on present switching technology [11]. Therefore, if the receiver response is fast enough, the loop length can be reduced and the reconfiguration time along with the steering speed of the proposed processor can also reach tens of nanoseconds. Nevertheless, several issues ought to be considered for practical applications, such as polarization-dependent loss or gain (PDL/PDG), filter sharpening, the gain-bandwidth product of the EDFA, and the optical signal-to-noise ratio (OSNR). Details of these issues of design and optimization will be discussed in a future contribution.

For receive-mode operation, the recirculating loop is used to compensate the time delay, as depicted in Figure 3. The RF signals from each antenna T/R element are modulated on different WDM optical channels using electro-optics modulators. As can be noted, the phase difference at the antenna elements depends on the target position. After the multiplexing stage, the WDM signal (carrying information about the relative RF delays) is input to the fiber loop. Thus, the phase delay between optical channels is compensated by the time delay introduced by the recirculating loop. After passing a specific number of times around the fiber loop, the signal is demodulated by a single photo-detector. The output power of the photo-detector depends on the corrected phase difference between the RF signals. Therefore, the output power is related to the target angular position via this phase difference [14].

A complete transceiver module can be designed, since both transmit and receive versions of the processor share the same PRL. In this case, the processor performs both tasks by using a single PRL in an asynchronized mode [15].

3. RESULTS

Several kinds of TTD elements can be used in this proposed recirculating loop to introduce a desired time delay between WDM channels. In our experiment, a fiber delay-line array is used. The experimental setup is shown in Figure 4. A set of 32 WDM channels are used with wavelengths ranging from 1530.34 to

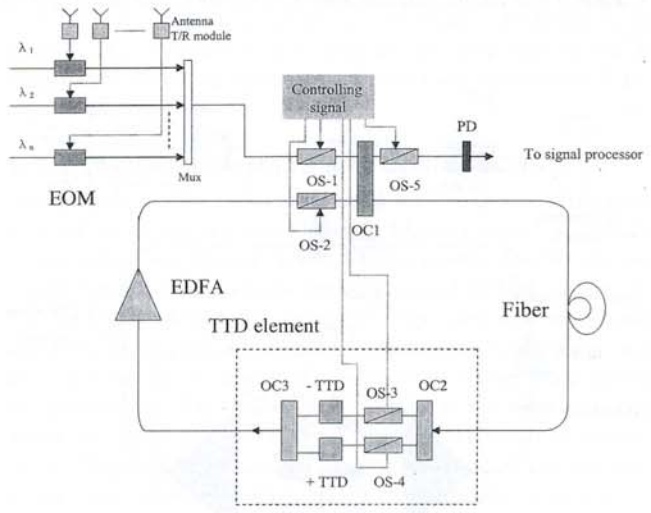

Figure 3 TTD optical beamformer architecture for receive mode based on a recirculating loop (OS: optical switch, OC: optical coupler, PD: photo detector; EOM: electro-optic modulator)

1553.48 nm with 100-GHz channel spacing. WDM channels are externally modulated with a 1.5-GHz signal and launched into the loop. Acousto-optic switches have a rise-time of 65 ns and an "on/off" time delay of 1 μs. Based on these performance parameters, the loop length is selected to be longer than 200 m in order to provide an adequate transit time and avoid overshooting. So, a spool of 20-km TW fiber with a 0.1-ps/km/nm^2 dispersion slope is used in our proof-of-concept experiment. Only two optical switches, OS1 and OS2, are implemented in the experimental apparatus. Therefore, the operation of OS5 is simulated by a trigger signal that controls data acquisition by the scope and the optical spectrum analyzer.

The structure of the TTD element is shown in detail in Figure 4. It includes two 32-channel AWG Mux and Demux, 32 fiber delay lines, and the same number of optical variable attenuators, which are used to equalize the power of the WDM channels after multiple loop passes. The delay between adjacent channels is set to 100 ps/loop (3-mm fiber-optical path increments). The maximum delay caused by the two AWGs, which is about 8 mm, is also taken into account. The number of recirculating loop passes is changed from 0 to 14 such that the relative delay between two adjacent channels varies from 0 to 1400 ps. In the experiment, the delay is measured for every two loop passes. Figure 5 shows the time delay, introduced by the PRL, between two adjacent channels (channels 1 and 2) after several loop passes. In each case, the time delay introduced by the PRL without the TTD elements is used as a reference. The delay is measured by a 4-GHz sampling scope triggered by the acquisition signal simulating OS5 and a triggering clock signal. As shown in Figure 5, the time delay varies linearly from 0 to 1400 ps when the number of loop passes changes from 0 to 14, as expected.

4. CONCLUSION

A novel high-speed, cost-effective, and programmable true-time-delay (TTD) processor for optical phased-array antennas based on a fiber-optic recirculating loop has been proposed. In comparison to other methods, this architecture significantly reduces the number of TTD components. Further simplification is also possible by replacing the array of delay lines along with WDM multiplexers with a single piece of high-dispersion fiber or a chirped Bragg grating (fixed or tunable). Therefore, the TTD device can be conveniently shared by all of the WDM channels (for the entire C-band). The reconfiguration speed of the PRL can reach tens of nanoseconds and is only limited by the response time of the optical switches and photodetectors. The proposed optical beamformer architecture is demonstrated as a proof-of-concept prototype. Furthermore, this beamformer is capable of simultaneously processing both receive and transmit RF beams in a single PRL network.

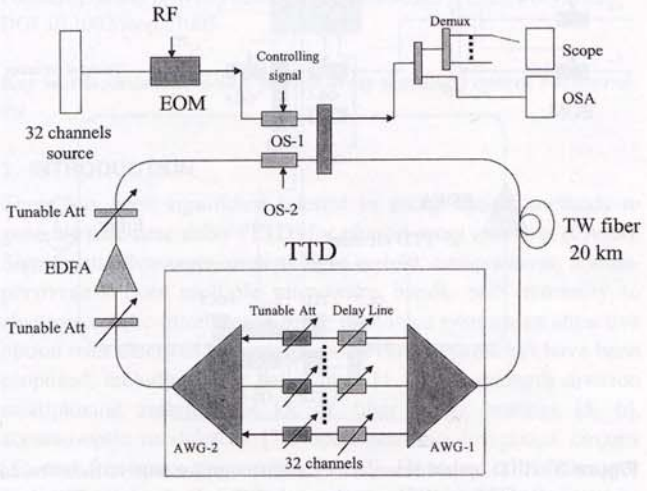

Figure 4 Experimental setup of the proposed optical beamformer

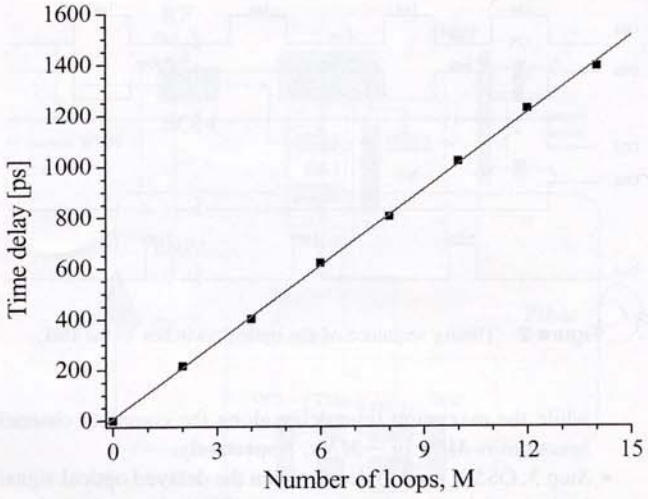

Figure 5 Time-delay measurements between two adjacent channels (channels 1 and 2) vs. the number of passes through the recirculating loop (parameter M)

ACKNOWLEDGMENT

This work was sponsored by the Office of Naval Research under contract no. N00014-00-0782.

REFERENCES

1. W. Ng and A.A. Watson, The first demonstration of an optically steered microwave phase array antenna using true time-delay, J Lightwave Technol 8 (1991), 1124–1131.
2. P.J. Matthews, M.Y. Frankel, and R.D. Esman, A wide-band fiber-optics true time-steered array receiver capable of multiple independent simultaneous beams, IEEE Photon Technol Lett 10 (1998), 722–724.
3. A.P. Goutzoulis, D.K. Davies, and J.M. Zomp, Hybrid electronics fiber optics wavelength-multiplexing system for true time delay steering of phase array antennas, Opt Eng 31 (1992), 2312–2322.
4. R. Taylor and S. Forrest, Steering for an optically-driven true-time delay phase-array antenna based on a broad-band coherent WDM architecture, IEEE Photon Technol Lett 10 (1998), 144–146.
5. B. Tsap, Y. Chang, H.R. Fetterman, A.F.J. Levi, D.A. Cohen, and I.L. Newberg, Phased-array optically controlled receiver using a serial feed, IEEE Photon Technol Tech Lett 10 (1998), 267–269.
6. S. Palit, S. Granieri, A. Siahmakoun, B. Black, K. Johnson, and J. Chestnut, Binary and ternary architectures for a two-channel 5-bit optical beamformer, Top Mtg Microwave Photon, 2002, pp. 273–276.
7. N.A. Riza, Acousto-optic liquid-crystal analog beam former for phase-array antennas, Appl Optics 33 (1994), 3712–3724.
8. L. Eldada, Laser-fabricated delay lines in GaAs for optically steered phase-array radar, J Lightwave Technol 13 (1995), 2034–2039.
9. Z. Fu, C. Zhou, and R.T. Chen, Waveguide-hologram-based wavelength-division multiplexed pseudo-analog true-time-delay module for wide-band phase array antennas, Appl Optics 38 (1999), 3053–3059.
10. A.M. Rader and B.L. Anderson, Demonstration of a linear optical true-time delay device by use of a microelectromechanical mirror array, Appl Optics 42 (2003), 1409–1416.
11. G.I. Papadimitriou, C. Papazoglou, and A.S. Pomportsis, Optical switching: Switch fabrication, techniques, and architectures, J Lightwave Technol 21 (2003), 384–405.
12. N.S. Bergano and C.R. Davidson, Circulating loop transmission experiments for the study of long-haul transmission systems using er-

bium-doped fiber amplifiers, J Lightwave Technol 13 (1995), 879–888.
13. S. Palit, M. Jaeger, S. Granieri, B. Black, J. Chestnut, and A. Siahmakoun, 5-bit programmable binary and ternary architectures for an optical transmit/receive beamformer, IEICE Trans Electron E86-C (2003), 1203–1208.
14. S. Granieri, M. Jaeger, and A. Siahmakoun, Multiple beam fiber-optic beamformer with binary array of delay lines, J Lightwave Technol 21 (2003), 3262–3272.
15. D. Tong and M. Wu, Transmit/receive module of multiwavelength optically controlled phased-array antennas, IEEE Photon Technol Lett 10 (1998), 1018–1020.

CIRCULARLY POLARIZED PROXIMITY-COUPLED MICROSTRIP ANTENNAS

Yi-Lung Lee, Tsair-Rong Chen, and Jeen-Sheen Row
Department of Electrical Engineering
National Changhua University of Education
Chang-Hua, Taiwan 500, R.O.C.

Received 2 March 2005

ABSTRACT: *A novel design for the production of circularly polarized radiation (CP) in proximity-fed microstrip antennas is presented. To achieve this circular-polarization design, the two orthogonal modes of the microstrip antenna are excited in series through the proximity coupling of an L-shaped open microstrip line. The experimental results show that the 3-dB axial-ratio CP bandwidth of the proposed design is increased by more than 30%, as compared to a conventional CP microstrip antenna of the same size. The details of the simulated and experimental results for the proposed design are presented and discussed.*
 Microwave Opt Technol Lett 46: 429–430, 2005; Published online in Wiley InterScience (www.interscience.wiley.com). DOI 10.1002/mop.21006

Key words: *microstrip antenna; circular polarization*

1. INTRODUCTION

For microstrip antennas, using proximity-coupled feed can provide the advantages of flexible impedance-matching design and easy integration with circuit devices, in comparison to the coaxial probe feed [1]. A conventional method of producing circularly polarized (CP) radiations for single-fed proximity-coupled microstrip antennas involves introducing a perturbation segment into the radiating patch. The perturbation segment can be designed by truncating the patch corners, using a nearly square patch [2] or embedding a centered cross slot on the patch [3]. In these designs, the two orthogonal resonant modes of the microstrip antenna are excited in parallel and have the same amplitude and 90° phase difference at the CP operating frequency. However, the obtained 3-dB axial-ratio CP bandwidth is limited, especially for the microstrip antenna with high quality factor. To effectively improve the CP bandwidth, the two orthogonal modes can be excited by two-port parallel-feed configuration integrated with a 90° hybrid coupler. However, the antenna area would be relatively larger and an additional transmission loss would certainly occur within the hybrid coupler, especially if it is fabricated on certain commercial laminates which have higher loss. In this paper, we propose a new design method to produce CP radiation for proximity-coupled microstrip antennas. The two orthogonal modes of the proposed design are excited in series, and the obtained CP bandwidth is obviously wider than that of the conventional single-fed CP microstrip antenna using the perturbation method.

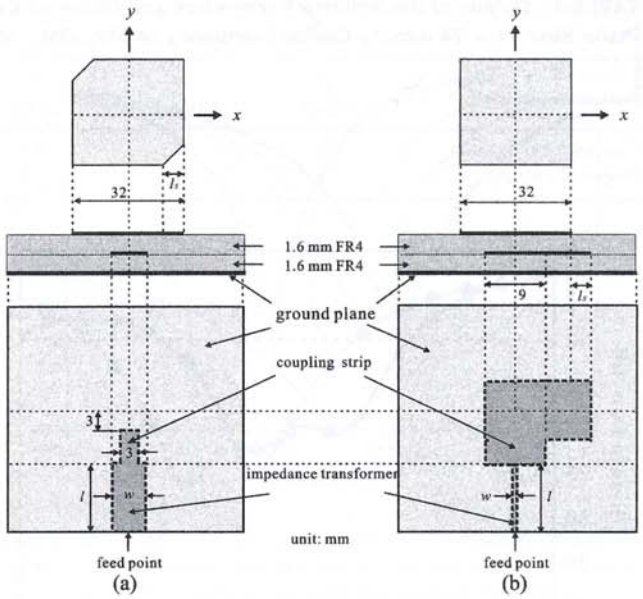

Figure 1 Geometries of the conventional and proposed CP microstrip antennas using proximity-coupled feed: (a) conventional antenna; (b) proposed antenna

2. ANTENNA DESIGN

The geometries of the conventional and proposed CP microstrip antennas using proximity-coupled feed are depicted in Figures 1(a) and 1(b), respectively. The radiating square patch with side length of 32 mm is fabricated on FR4 substrate of thickness 1.6 mm and relative permittivity 4.4. The microstrip feed line is printed on FR4 substrate of the same thickness, and is composed of a coupling strip and a quarter-wavelength impedance transformer. The coupling strips are a y-directed straight strip for the conventional design and an L-shaped strip for the proposed design. Therefore, the two orthogonal modes of the proposed design are excited in series through the proximity coupling of the L-shaped strip, as opposed to the parallel type of the conventional design, and it is found that the optimum axial ratio can be obtained by tuning l_s. In addition, the impedance matching of the proposed design is achieved by selecting the proper characteristic impedance of the impedance transformer.

3. EXPERIMENTAL RESULTS AND CONCLUSIONS

The prototypes for the conventional and proposed proximity-coupled microstrip antennas shown in Figure 1 were respectively implemented and studied. Their detailed design dimensions and obtained experimental results are summarized in Table 1. Figures 2(a) and 2(b) present the measured return loss and axial ratio against frequency for the two antenna prototypes, respectively, and the simulated results carried out using IE3D software are shown for comparison. The discrepancies between the simulated and measured results may be due to an error in the substrate permittivity. Observing the measured results, both studied antenna prototypes have almost the same 10-dB input-impedance bandwidth (~6.5%); however, the 3-dB axial-ratio CP bandwidth of the proposed antenna has an increase of 35%, as compared to that of the conventional antenna. It was also found that the proposed CP series feed mechanism can be applied to wideband antennas, such